Low Oxidation State Silicon Clusters – Synthesis and Structure of [NHC^{Dipp}Cu(η^4-Si$_9$)]$^{3-}$

Felix. S. Geitner,[a] Thomas. F. Fässler[*b]

[*b]   Prof. Dr. Thomas. F. Fässler, Department of Chemistry, Technische Universität München

         Lichtenbergstraße 4, 85747 Garching/München, Germany

[a]   Felix S. Geitner, WACKER Institute for Silicon Chemistry and Departement of Chemistry, Technische

         Universität München Lichtenbergstraße 4, 85747 Garching/München, Germany

Content

1. Experimental Section

1.1 General:

All manipulations were carried out under a purified argon atmosphere using standard Schlenk and glove box techniques. $K_{12}Si_{17}$, $K_6Rb_6Si_{17}$ and $Rb_{12}Si_{17}$ were prepared by fusion of stoichiometric amounts of the elements in sealed tantalum ampoules and stored under argon atmosphere. Imidazolium salts and NHC*M*Cl (*M*: Cu, Ag, Au; NHC: NHC^{Dipp}, NHC^{Mes} and NHC^{iPr}) were prepared according to modified literature procedures.[1-4] [2.2.2-crypt] was dried *in vacuo* overnight. Liquid ammonia was dried and stored over sodium metal. Anhydrous pyridine (VWR) was stored over molecular sieves prior to usage. All other solvents were obtained from a MBraun Grubbs apparatus.

1.2 Syntheses

1a: $K_{12}Si_{17}$ (71 mg, 0.075 mmol, 1 eq.), NHC^{Dipp}CuCl (36.5 mg, 0.075 mmol, 1 eq.) and [2.2.2-crypt] (52 mg, 0.135 mmol, 1.86 eq.) were weighted into a Schlenk tube. Addition of ammonia (approximately 2 mL) led to the formation of a deep red suspension. The samples were stored in a freezer at -70 °C. Compound **1a** crystallizes as red block-shaped crystals in approx. 35 % yield (estimated by the amount of red crystalline material found in the sample).

1b: $K_6Rb_6Si_{17}$ (92 mg, 0.075 mmol, 1 eq.), NHC^{Dipp}CuCl (36.5 mg, 0.075 mmol, 1 eq.) and [2.2.2-crypt] (52 mg, 0.135 mmol, 1.86 eq.) were weighted into a Schlenk tube. Addition of ammonia (approximately 2 mL) led to the formation of a deep red suspension. The samples were stored in a freezer at -70 °C. Compound **1b** crystallizes as red block-shaped crystals in approx. 30 % yield (estimated by the amount of red crystalline material found in the sample).

1c: $Rb_{12}Si_{17}$ (113 mg, 0.075 mmol, 1 eq.), NHC^{Dipp}CuCl (36.5 mg, 0.075 mmol, 1 eq.) and [2.2.2-crypt] (52 mg, 0.135 mmol, 1.86 eq.) were weighted into a Schlenk tube. Addition of ammonia (approximately 2 mL) led to the formation of a deep red suspension. The samples were stored in a freezer at -70 °C. Compound **1c** crystallizes as red block-shaped crystals in approx. 30 % yield (estimated by the amount of red crystalline material found in the sample).

Reactions of $K_{12}Si_{17}$ with NHC^{Dipp}*M*Cl (*M*: Ag, Au)

$K_{12}Si_{17}$ (71 mg, 0.075 mmol, 1 eq.), NHC^{Dipp}*M*Cl (40.0 mg (*M*: Ag); 46.5 mg (*M*: Au), 0.075 mmol, 1 eq.) and [2.2.2-crypt] (52 mg, 0.135 mmol, 1.86 eq.) were weighted into a Schlenk tube. Addition of ammonia (approximately 2 mL) led to the formation of deep red suspensions. The samples were stored in a freezer at -70 °C. After 3 months, bright orange block-shaped were found, which were identified as [K(2.2.2-crypt)]$_3$[Si$_9$] by SC-XRD.[5]

Reactions of K$_{12}$Si$_{17}$ with NHC-CuCl (NHC: NHC^{Mes}, NHC^{iPr})

K$_{12}$Si$_{17}$ (71 mg, 0.075 mmol, 1 eq.), NHC-CuCl (30.3 mg (NHC: NHC^{Mes}); 18.0 mg (NHC: NHC^{iPr}), 0.075 mmol, 1 eq.) and [2.2.2-crypt] (52 mg, 0.135 mmol, 1.86 eq.) were weighted into a Schlenk tube. Addition of ammonia (approximately 2 mL) led to the formation of deep red suspensions. The samples were stored in a freezer at -70 °C overnight. Subsequently, ammonia was removed and the obtained solids were extracted with pyridine, yielding deep red suspensions. ESI-MS examinations of these solids revealed the attachment of the respective [Cu-NHC]$^+$ moieties to the [Si$_9$] clusters. Selected areas of the acquired ESI-MS spectra are pictured in Figure SI 10.

1.3 Single Crystal Structure Determination

Crystal structure determination: The thermally very unstable, air and moisture sensitive crystals of **1a**-**1c** were transferred from the mother liquor into cooled perfluoroalkylether oil under a cold N$_2$ gas stream. For single crystal data collection, the single crystals were fixed on a glass capillary and positioned in a 120 K cold N$_2$ gas stream using the crystal cap system. Single crystal data collection was performed at an Oxford-Diffraction Xcalibur3 diffractometer (Mo$_{K\alpha}$ radiation). Structures were solved by Direct Methods (SHELXS-2014) and refined by full-matrix least-squares calculations against F^2 (SHELXL-2014).[6] Supplementary crystallographic data for this paper has been deposited with the Cambridge Structural database and are available free of charge via www.ccdc.cam.ac.uk/data_request/cif. In compound **1b** free refinement of the K and Rb postions gave a K/Rb ratio of 3.15/2.85. Furthermore, one Rb$^+$ cation (Rb1) is disordered and has been refined on split positions. Regarding compound **1c** only small crystals, which did not diffract very good were obtained. Hence, for **1c** only the unit cell volume and a crude structural model, confirming its similarity to compounds **1a** and **1b**, could be determined.

Table SI 1: Crystallographic data for compounds **1a** and **1b**.

Compound	1a	1b
formula	$Si_{18}Cu_2C_{108}H_{258}N_{10}O_{18}K_6 \cdot 26NH_3$	$Si_{18}Cu_2C_{108}H_{258}N_{10}O_{18}K_{3.15}Rb_{2.85} \cdot 26NH_3$
crystal size	0.5 x 0.45 x 0.35	0.35 x 0.30 x 0.15
fw (g·mol^{-1})	3216.79	3348.94
space group	$P\bar{1}$	$P\bar{1}$
a (Å)	17.1066(3)	17.1296(4)
b (Å)	18.1573(3)	18.1554(3)
c (Å)	30.8056(5)	30.7960(5)
α (deg)	87.076(1)	86.899(1)
β (deg)	81.339(2)	81.149(2)
γ (deg)	65.383(2)	65.729(2)
V (Å^3)	8598.9(3)	8626.5(3)
Z	2	2
T (K)	120(2)	120(2)
λ (Å)	0.71073	0.71073
ρ_{calcd} (g·cm^{-3})	1.242	1.289
μ (mm^{-1})	0.580	1.308
collected reflections	238725	205952
independent reflections	33153	33838
R_{int} / R_δ	0.0780 / 0.0861	0.0943 / 0.1597
parameters / restraints	1709 / 30	1726 / 61
R_1 [$I > 2\sigma(I)$ / all data]	0.0418 / 0.0766	0.0443 / 0.1068
wR_2 [$I > 2\sigma(I)$ / all data]	0.0962 / 0.1036	0.0967 / 0.1074
goodness of fit	0.900	0.823
max./min. diff. el. density (e / Å^{-3})	0.99/ -0.59	1.38/-0.78
CCDC	1566679	1566680

Table SI 2: Cell parameters and cell volume of compound **1c**.

Compound	1c
a (Å)	17.139(3)
b (Å)	18.180(4)
c (Å)	30.822(6)
α (deg)	87.02(3)
β (deg)	81.27(3)
γ (deg)	65.86(3)
V (Å³)	8661(4)

Table SI 3: Selected bond lengths of cluster **A** in compounds **1a** and **1b**:

1a-A		1b-A	
Bond	Distance in [Å]	Bond	Distance in [Å]
Cu1-Si6	2.4195(9)	Cu1-Si6	2.425(1)
Cu1-Si7	2.4186(9)	Cu1-Si7	2.417(1)
Cu1-Si8	2.4238(8)	Cu1-Si8	2.419(1)
Cu1-Si9	2.4321(9)	Cu1-Si9	2.436(1)
Cu1-C1	1.925(3)	Cu1-C1	1.931(4)
Si1-Si2	2.420(1)	Si1-Si2	2.422(2)
Si1-Si3	2.445(1)	Si1-Si3	2.446(2)
Si1-Si4	2.422(1)	Si1-Si4	2.416(2)
Si1-Si5	2.464(1)	Si1-Si5	2.460(2)
Si2-Si3	2.664(1)	Si2-Si3	2.663(2)
Si2-Si5	2.624(1)	Si2-Si5	2.622(2)
Si2-Si6	2.420(1)	Si2-Si6	2.421(2)
Si2-Si9	2.418(1)	Si2-Si9	2.420(2)
Si3-Si4	2.651(1)	Si3-Si4	2.644(2)
Si3-Si6	2.423(1)	Si3-Si6	2.422(2)
Si3-Si7	2.412(1)	Si3-Si7	2.412(2)
Si4-Si5	2.592(1)	Si4-Si5	2.595(2)
Si4-Si7	2.428(1)	Si4-Si7	2.425(2)
Si4-Si8	2.414(1)	Si4-Si8	2.410(2)
Si5-Si8	2.422(1)	Si5-Si8	2.416(2)
Si5-Si9	2.426(1)	Si5-Si9	2.426(2)
Si6-Si7	2.560(1)	Si6-Si7	2.545(2)
Si6-Si9	2.587(1)	Si6-Si9	2.585(2)
Si7-Si8	2.606(1)	Si7-Si8	2.614(2)
Si8-Si9	2.569(1)	Si8-Si9	2.568(2)

Table SI 4: Selected bond lengths of cluster **B** in compounds **1a** and **1b**:

1a-B		1b-B	
Bond	**Distance in [Å]**	**Bond**	**Distance in [Å]**
Cu2-Si15	2.4459(9)	Cu2-Si15	2.456(1)
Cu2-Si16	2.4243(9)	Cu2-Si16	2.415(1)
Cu2-Si17	2.4590(9)	Cu2-Si17	2.461(1)
Cu2-Si18	2.4283(9)	Cu2-Si18	2.424(1)
Cu2-C4	1.953(3)	Cu2-C4	1.943(4)
Si10-Si11	2.444(1)	Si10-Si11	2.442(2)
Si10-Si12	2.433(1)	Si10-Si12	2.434(2)
Si10-Si13	2.445(1)	Si10-Si13	2.451(2)
Si10-Si14	2.427(1)	Si10-Si14	2.428(2)
Si11-Si12	2.638(1)	Si11-Si12	2.645(2)
Si11-Si14	2.647(1)	Si11-Si14	2.644(2)
Si11-Si15	2.433(1)	Si11-Si15	2.427(2)
Si11-Si18	2.436(1)	Si11-Si18	2.432(2)
Si12-Si13	2.642(1)	Si12-Si13	2.635(2)
Si12-Si15	2.437(1)	Si12-Si15	2.438(2)
Si12-Si16	2.418(1)	Si12-Si16	2.415(2)
Si13-Si14	2.652(1)	Si13-Si14	2.657(2)
Si13-Si16	2.412(1)	Si13-Si16	2.408(2)
Si13-Si17	2.427(1)	Si13-Si17	2.425(2)
Si14-Si17	2.425(1)	Si14-Si17	2.425(2)
Si14-Si18	2.418(1)	Si14-Si18	2.424(2)
Si15-Si16	2.574(1)	Si15-Si16	2.568(2)
Si15-Si18	2.560(1)	Si15-Si18	2.545(2)
Si16-Si17	2.557(1)	Si16-Si17	2.553(2)
Si17-Si18	2.575(1)	Si17-Si18	2.574(2)

Table SI 5: Comparison of bond lengths and angles in compounds **1a** and **1b**:

Compound	1a		1b	
Cluster	**1a-A**	**1a-B**	**1b-A**	**1b-B**
d(Si-Si); shortest [Å]	2.412(1)	2.412(1)	2.410(2)	2.408(2)
d(Si-Si); longest [Å]	2.664(1)	2.652(1)	2.663(2)	2.657(2)
d(Cu-Si); mean [Å]	2.4235(9)	2.4394(9)	2.424(1)	2.439(1)
d(Cu-C$_{carbene}$) [Å][a]	1.925(3)	1.953(3)	1.931(4)	1.943(4)
csp-Cu-C$_{carbene}$ [°][b]	178.54(2)	176.82(4)	178.02(3)	175.96(8)
torsion angle α [°][c]	179.80(2)	179.90(2)	179.98(2)	179.70(2)
d2/d1[d]	1.00	1.02	1.00	1.02

[a] d(Cu-C$_{Carbene}$): Distance between Cu$^+$ and the respective carbene carbon atoms C1 or C4. [b] csp: centre of gravity of the square open plane of [Si$_9$], which coordinates to the [Cu-NHC]$^+$ fragment. [c] For clusters **A**: Si6-Si7-Si8-Si9; for clusters **B**: Si15-Si16-Si17-Si18. [d] Relation of the diagonal lengths of the square open plane of the [Si$_9$] clusters coordinating to [Cu-NHC]$^+$.
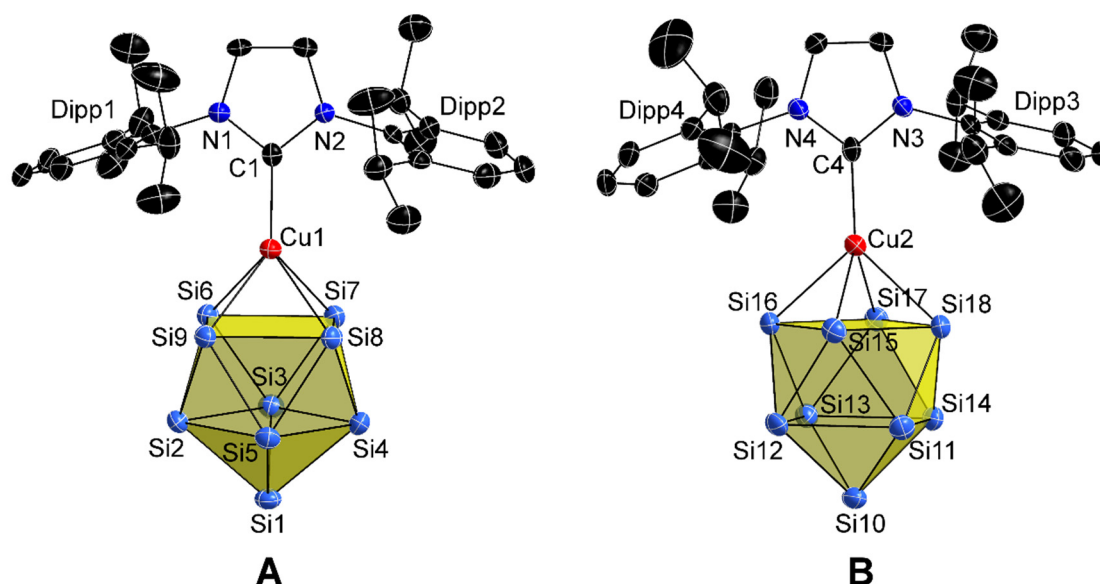
Figure SI 1: Full ellipsoid molecular structures of the two crystallographically different [NHC^{Dipp}Cu(η^4-Si$_9$)]$^{3-}$ clusters in compound **1a**. Ellipsoids are shown at a 50 % probability level. Hydrogen atoms and solvent molecules are omitted for clarity.
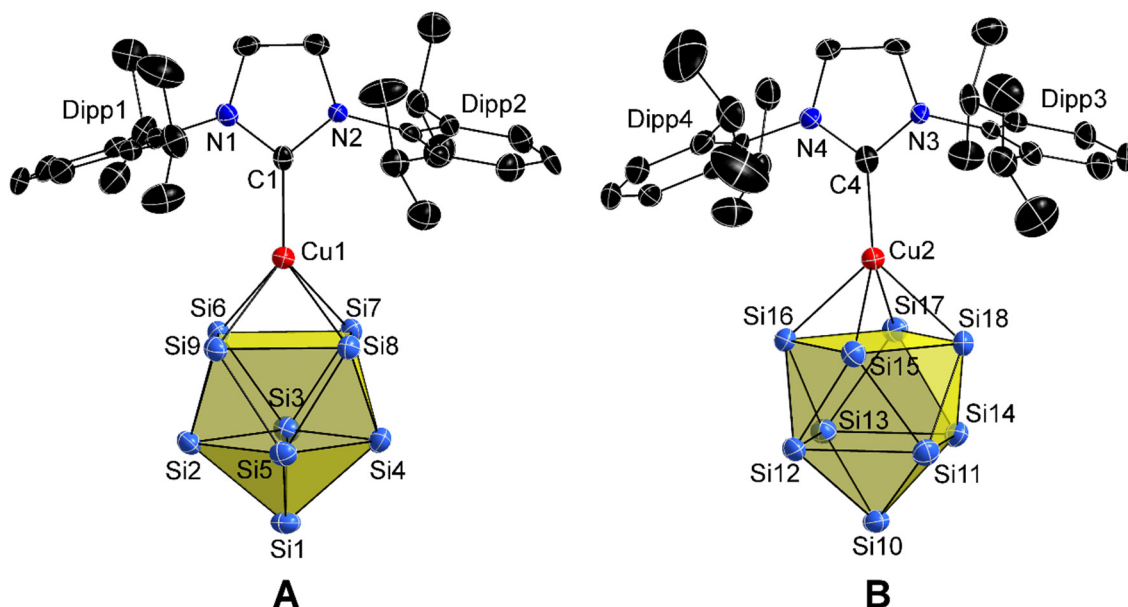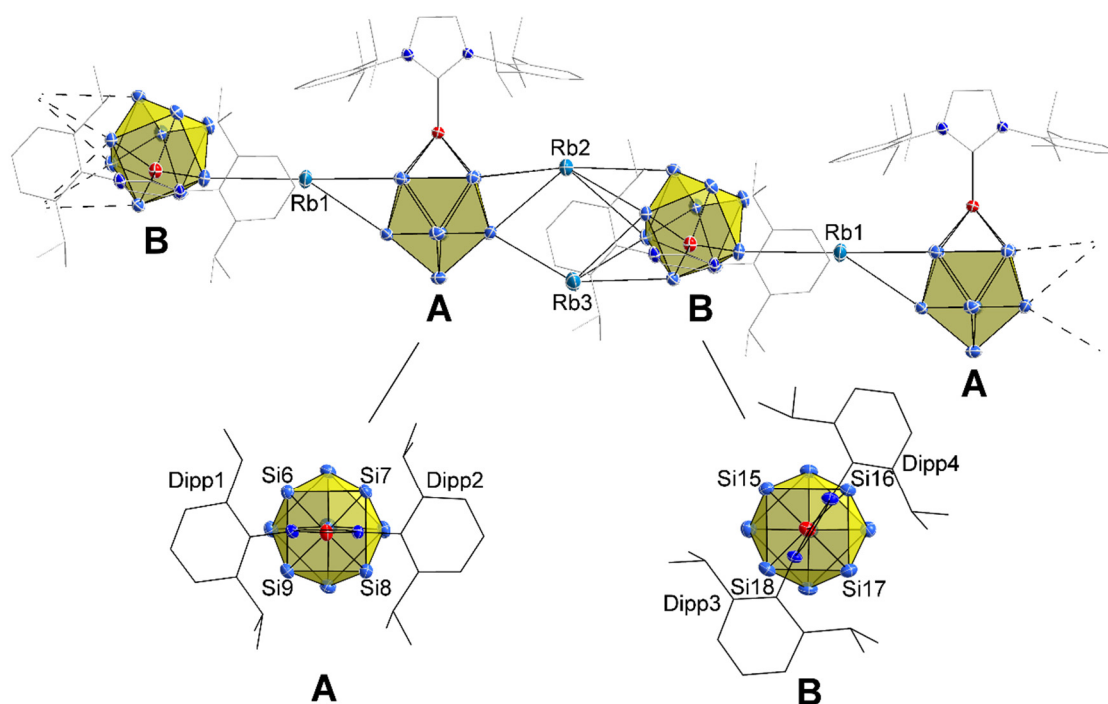
Figure SI 2: Full ellipsoid molecular structures of the two crystallographically different $[NHC^{Dipp}Cu(\eta^4\text{-}Si_9)]^{3-}$ clusters in compound **1b**. Ellipsoids are shown at a 50 % probability level. Hydrogen atoms and solvent molecules are omitted for clarity.

Figure SI 3: Top: Linear strands of Rb^+ connected $[NHC^{Dipp}Cu(\eta^4\text{-}Si_9)]^{3-}$ clusters **A** and **B** in **1b**. Rb-Si distances range between 3.467(1) Å (Rb1-Si2) and 3.872(1) Å (Rb3-Si12). Ellipsoids are shown at a 50 % probability level. For clarity protons and solvent molecules are omitted and carbon atoms are pictured as grey wire sticks. Bottom: Different orientations of $[Cu\text{-}NHC^{Dipp}]^+$ moieties towards the $[Si_9]^{4-}$ core in **A** and **B**.
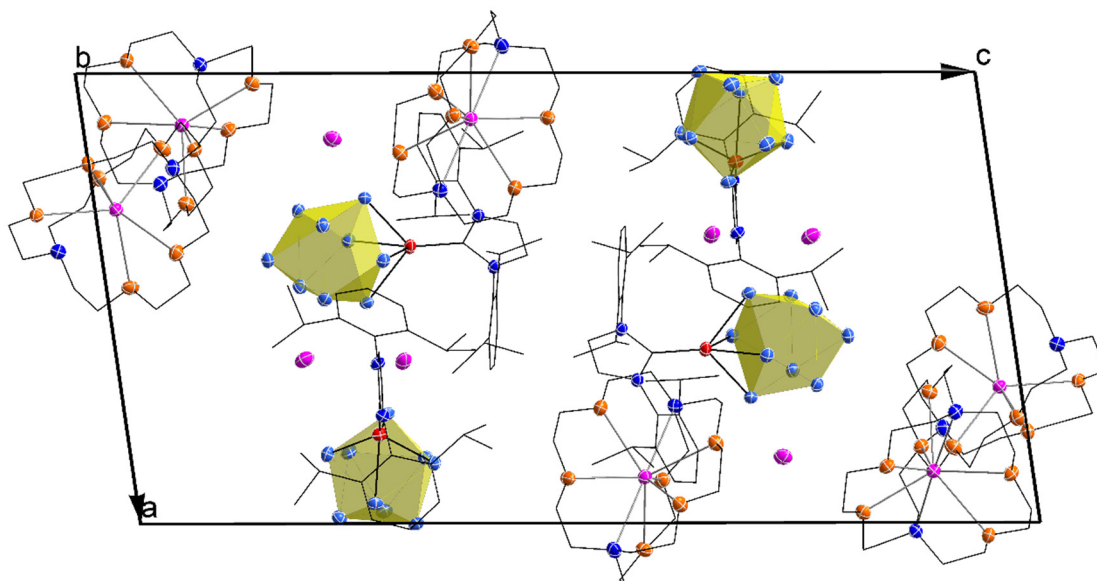
Figure SI 4 Unit cell of compound **1a**. Ellipsoids are shown at a 50 % probability. For clarity protons and solvent molecules are omitted and carbon atoms are pictured as grey wire sticks. Si atoms (bright blue), Cu atoms (red), K atoms (pink) N atoms (dark blue), O atoms (orange).
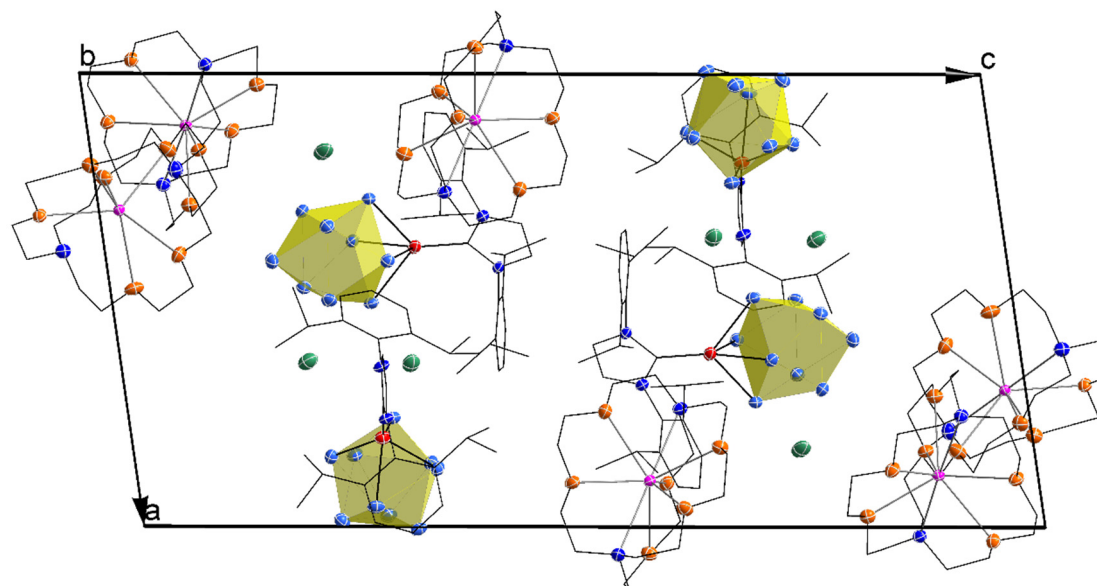

Figure SI 5 Unit cell of compound **1b**. Ellipsoids are shown at a 50 % probability. For clarity protons and solvent molecules are omitted and carbon atoms are pictured as grey wire sticks. Si atoms (bright blue), Cu atoms (red), Rb atoms (green), K atoms (pink), N atoms (dark blue), O atoms (orange).

1.4 NMR Spectroscopy

Subsequent to removal of NH_3 (l) from the reaction mixture, the orange-brownish residue was extracted with acetonitrile-d_3 and filtered to remove remaining solids. NMR spectra were acquired on a Bruker Avance Ultrashield 400 MHz spectrometer. The ^{1}H NMR spectra were calibrated using the residual proton signal of the used deuterated solvents. Chemical shifts are reported in parts per million (ppm) relative to TMS, with the residual solvent peak serving as internal reference.[7] Abbreviations for signal multiplicities are: doublet (d), heptet (h) or multiplet (m). For the time dependent studies, the sample was either stored at room-temperature or at -32 °C. In case of the low temperature examinations the J-Young tube was placed in an Argon-filled Schlenk tube in a freezer in between the single measurements.
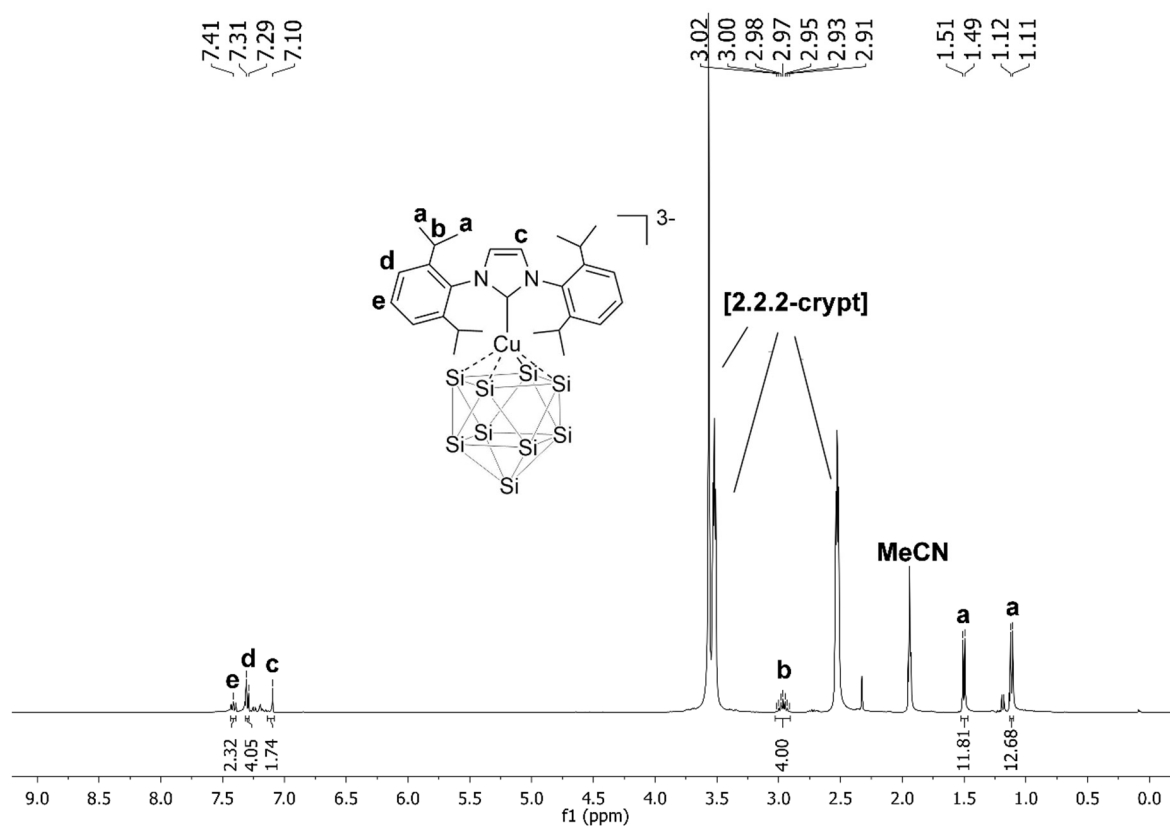

Figure SI 6 ^{1}H NMR spectrum of $[NHC^{Dipp}Cu(\eta^4\text{-}Si_9)]^{3-}$ (**1**) in MeCN-d_3.

^{1}H NMR (400 MHz, 298 K, MeCN-d_3): δ [ppm] = 7.43-7.39 (m, 2H, CH$_{Ph(p)}$), 7.32-7.29 (m, 4H, CH$_{Ph(m)}$), 7.10 (s, 2H, CH$_{Im}$), 2.97 (h, $^3J_{HH}$ = 6.8 Hz, 4H, CH$_{iPr}$), 1.49 (d, $^3J_{HH}$ = 6.8 Hz, 12H, Me$_{iPr}$), 1.11 (d, $^3J_{HH}$ = 6.8 Hz, 12H, Me$_{iPr}$). The intensity of the doublet at 1.11 ppm is slightly increased, due to an overlap of this signal with one of the respective signals of free carbene NHC^{Dipp}, which was present in small amounts in the sample.
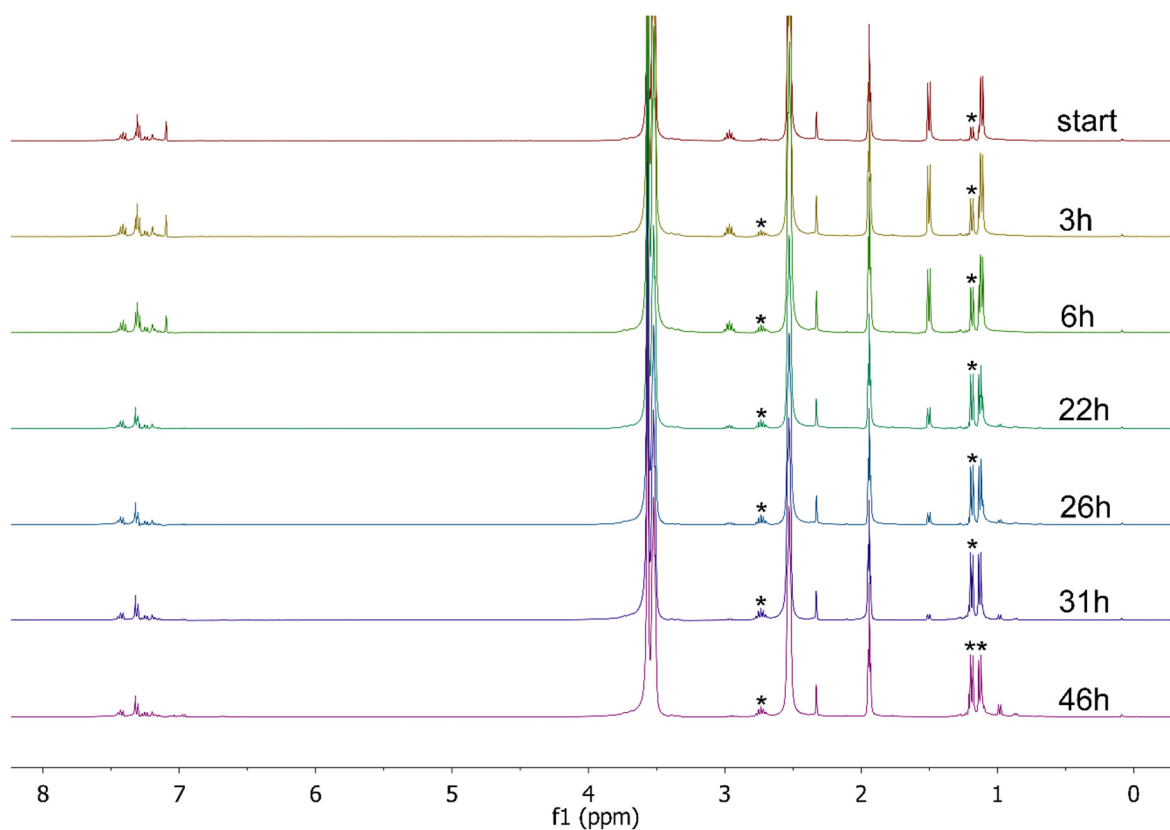
Figure SI 7 Time dependant ^{1}H NMR examination of [NHC^{Dipp}Cu(η^4-Si$_9$)]$^{3-}$ (**1**) in MeCN-d$_3$ at room temperature, revealing the complete degradation of **1** within 46 h. Characteristic signals of the free carbene are marked with (*).
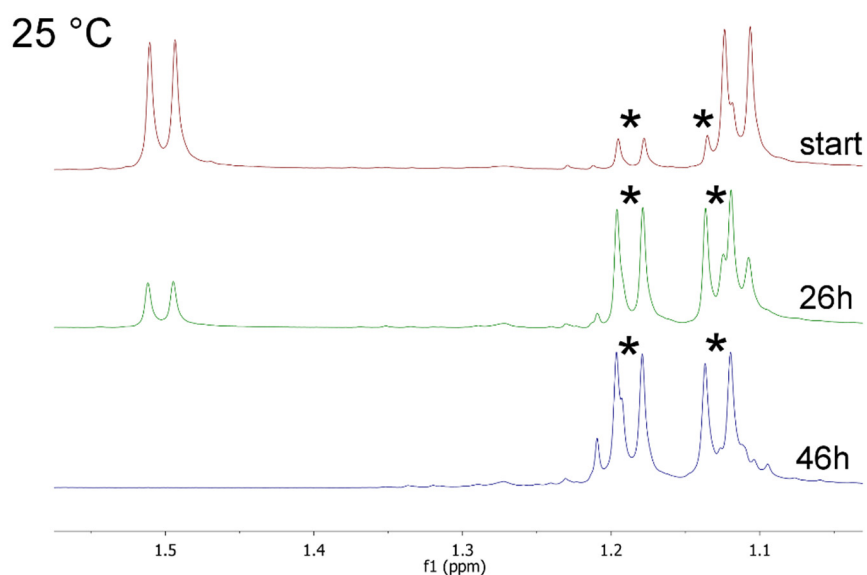

Figure SI 8 Selected area of time dependant ^{1}H NMR examination of [NHC^{Dipp}Cu(η^4-Si$_9$)]$^{3-}$ (**1**) in MeCN-d$_3$ at room temperature, revealing the complete degradation of **1** within 46 h. Characteristic signals of the free carbene are marked with (*).
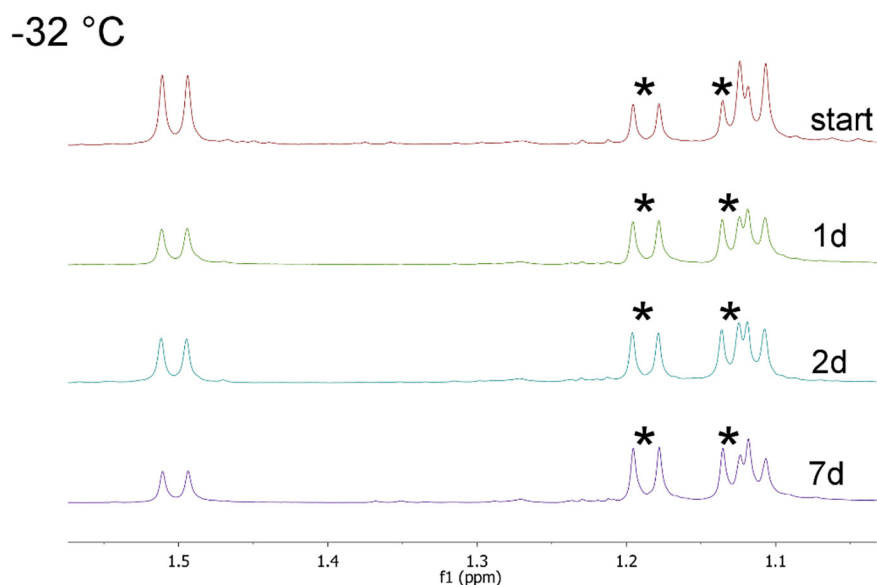
Figure SI 9 Selected area of time dependant ^{1}H NMR examination of [NHC$^{\text{Dipp}}$Cu(η^4-Si$_9$)]$^{3-}$ (**1**) in MeCN-d$_3$ at -32 °C, revealing the stability of **1** at low temperature. Slow progress of the reaction can be assigned to the short exposure to room temperature during the measurements. Characteristic signals of the free carbene are marked with (*).

1.5 Electron Spray Ionization Mass Spectrometry (ESI-MS)

Subsequent to removal of NH$_3$ (l) from the reaction mixture, the orange-brownish residue was dissolved in pyridine and filtered to remove remaining solids. Aliquots of this solution were diluted with pyridine to obtain suitable concentration for ESI-MS examinations. The measurements were performed on a HCT (*Bruker Corp.*). Analysis of the data occurred using the program Bruker Compass Data Analysis 4.0 SP 5 (*Bruker Corp.*). The dry gas temperature was adjusted to 300°C and the injection speed to 240 µL/s. Visualization of the spectra occurred with the programs OriginPro 2016G (*Origin Lab Corp.*) and Excel 2016 (*Microsoft Corp.*).

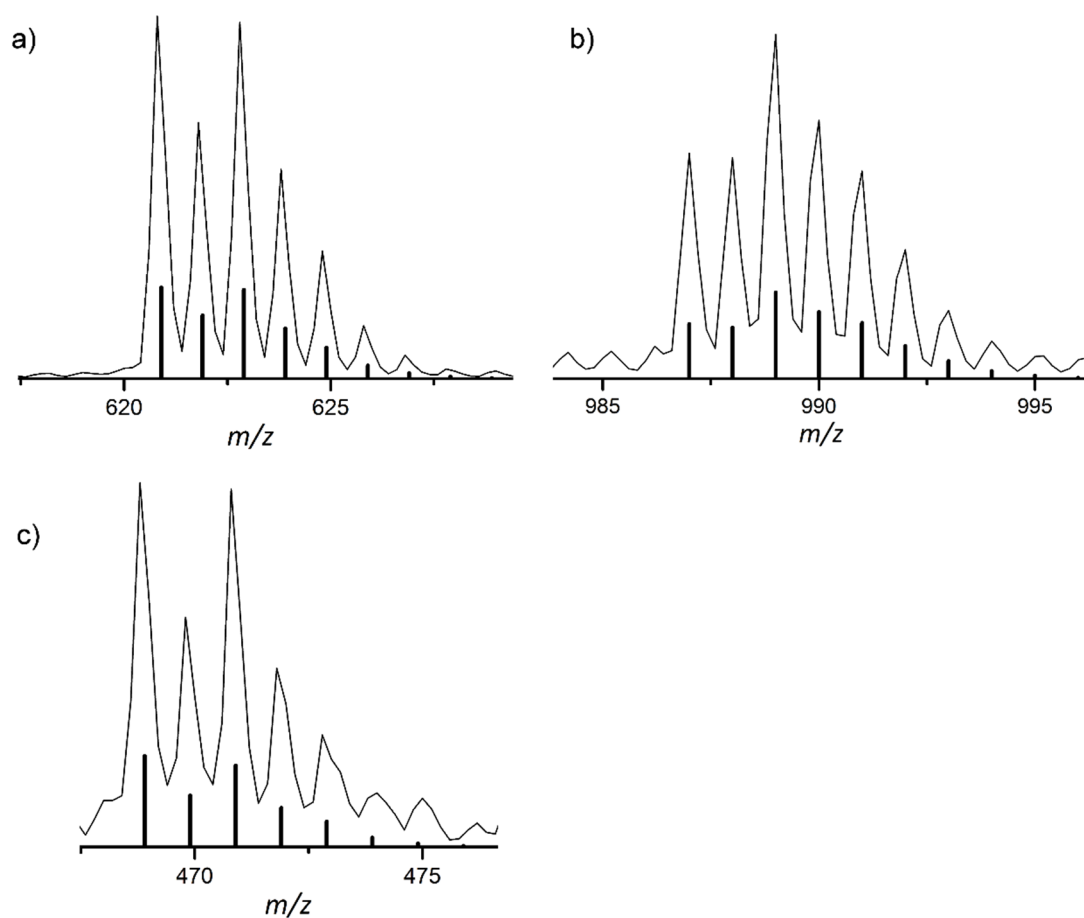**Figure SI 10** ESI-MS spectra of a) $\{[NHC^{Mes}CuSi_9]^{3-} + 2H^+\}^-$, b) $\{[(NHC^{Mes}Cu)_2Si_9]^{2-} + H^+\}^-$ and c) $\{[NHC^{iPr}Cu\text{-}Si_9]^{3-} + 2H^+\}$. All spectra were acquired in negative ion mode; a), b) (4500 V, 300 °C) and c) (3500 V, 300 °C).

Furthermore, MS-MS fragmentation experiments were carried out for $[NHC^{Dipp}Cu(\eta^4\text{-}Si_9)]^{3-}$ (**1**), resulting in the cleavage of the Cu-NHC^{Dipp} bonds for both originally monitored species at m/z 705.0 $\{[NHC^{Dipp}CuSi_9)]^{3-} + 2H^+\}^-$ (Figure SI 11) and m/z 1155.2 $\{[(NHC^{Dipp}Cu)_2Si_9]^{2-} + H^+\}^-$ (Figure SI 12). By contrast the Cu-Si bonds and the $[Si_9]$ cages stayed intact in these examinations.
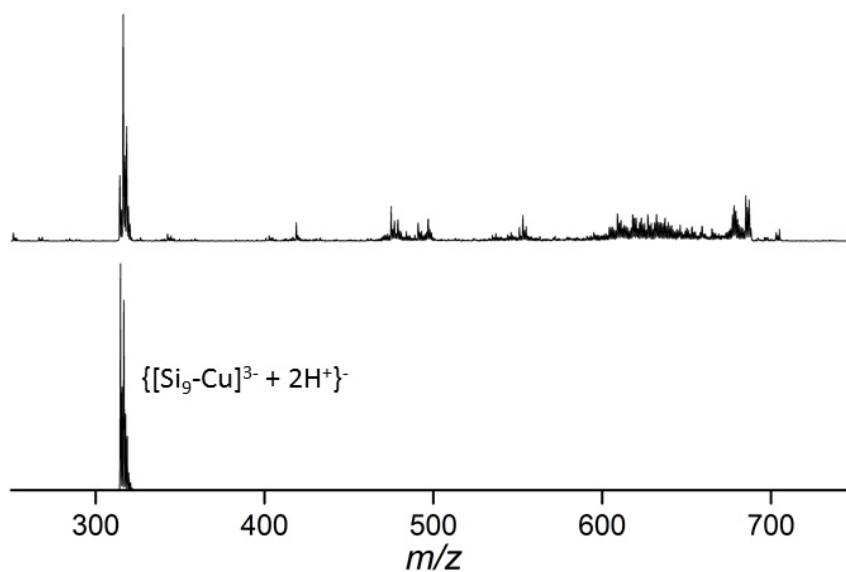
Figure SI 11: MS-MS fragmentation spectrum of $\{[NHC^{Dipp}CuSi_9)]^{3-} + 2H^+\}^-$ (top) and calculated reference spectrum of $\{[Si_9\text{-}Cu]^{3-} + 2H^+\}^-$ (bottom).
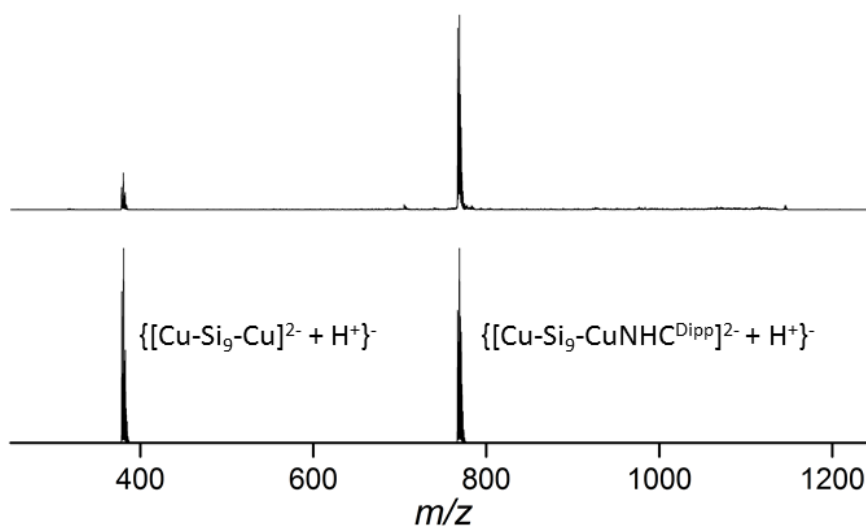

Figure SI 12: MS-MS fragmentation spectrum of $\{[(NHC^{Dipp}Cu)_2Si_9]^{2-} + H^+\}^-$ (top) and calculated reference spectra of $\{[Cu\text{-}Si_9\text{-}Cu]^{2-} + H^+\}^-$ and $\{[Cu\text{-}Si_9\text{-}CuNHC^{Dipp}]^{2-} + H^+\}^-$ (bottom).

References

1. L. Hintermann, *Beilstein J. Org. Chem.*, 2007, **3**, 22.
2. O. Santoro, A. Collado, A. M. Z. Slawin, S. P. Nolan and C. S. J. Cazin, *Chem. Commun.*, 2013, **49**, 10483.
3. P. de Frémont, N. M. Scott, E. D. Stevens, T. Ramnial, O. C. Lightbody, C. L. B. Macdonald, J. A. C. Clyburne, C. D. Abernethy and S. P. Nolan, *Organometallics*, 2005, **24**, 6301.
4. A. Collado, A. Gomez-Suarez, A. R. Martin, A. M. Z. Slawin and S. P. Nolan, *Chem. Commun.*, 2013, **49**, 5541.
5. J. M. Goicoechea and S. C. Sevov, *Journal of the American Chemical Society*, 2004, **126**, 6860.
6. G. Sheldrick, *Acta Cryst. Sect. C*, 2015, **71**, 3.
7. G. R. Fulmer, A. J. M. Miller, N. H. Sherden, H. E. Gottlieb, A. Nudelman, B. M. Stoltz, J. E. Bercaw and K. I. Goldberg, *Organometallics*, 2010, **29**, 2176.